Materials Advances

ROYAL SOCIETY OF CHEMISTRY

PAPER

View Article Online
View Journal | View Issue

Cite this: *Mater. Adv.*, 2025, 6, 8541

Engineering shootable mycelium-bound composites (MBCs) as living building materials

Xue Brenda Bai, [a] Ellen W. van Wijngaarden, [bc] Meredith N. Silberstein *[bc] and Marta H. Wisniewska*[a]

Received 19th June 2025,
Accepted 24th September 2025

DOI: 10.1039/d5ma00656b

rsc.li/materials-advances

The construction industry greatly contributes to global energy consumption (36%), CO_2 emissions (37%), and solid waste (35%), driving interest in bio-based materials such as mycelium-bound composites (MBCs) to reduce the environmental impact. MBCs combine fungal mycelium with agricultural waste to create lightweight, insulating structures with low energy requirements for manufacturing. However, current MBC fabrication methods – typically mold-based or limited scale extrusion-based 3D printing – constrain efficiency, geometric freedom, and scalability for building applications. Here, we introduce a novel shootable MBC formulation that supports vertical deposition by harnessing psyllium husk gel, a plant-derived polysaccharide binder chosen for its availability and unique rheology-modifying capacity. By tuning gel concentration, processing, and mixing protocols, we engineer MBC mixtures with tailored pre-growth mechanical properties that permit stable deposition *via* shooting. Through systematic characterization, we provide new insights into how material treatment methods influence both process and final MBC properties. Engineered formulations demonstrated consistent shootability over a span of 50 minutes with minimal material loss (<10%), with robust mycelium growth at both the surface and throughout the cross section. To illustrate the construction potential of shootable MBC formulations, we use concrete-inspired spray techniques to shoot a meter-scale MBC layer, unlocking a new paradigm in MBC design that is scalable, form-flexible, and time-efficient.

1. Introduction

The construction industry is a major contributor to environmental degradation through intensive resource extraction, carbon emissions, and long-lived waste, highlighting the urgent need for sustainable alternatives to traditional building materials.[1] Mycelium—the vegetative network of fungi—comprises a complex network of branching hyphae that function as a natural binding agent.[2] Mycelium-bound composites (MBCs), resulting from mycelial branches grown on organic substrates, especially lignocellulosic feedstocks (*e.g.* hemp, straw, or flax), could be a sustainable alternative to conventional building materials.[3] This unique as-grown lightweight composite can be applied in the building industry, for example, as thermal insulation,[4] acoustic panels,[5] or architectural installations.[6] To fabricate these products, customized molds are filled with lignocellulosic–mycelium mixtures, prepared using lignocellulosic biomass and mycelium spawn, and left to complete colonization, which is subsequently stopped by drying.[7] However, the loose particle- or fiber-based nature of MBCs during the fabrication process (before the hyphal network has grown) is challenging for use on inclined surfaces and complex geometries. It is difficult to control the shape due to the lack of cohesion, requiring labor-intensive manual packing of MBCs within molds for manufacturing building materials.[8]

Extrusion-based 3D printing of MBCs has emerged as a promising alternative to conventional molding processes, enabling greater geometric versatility and automated fabrication.[9] However, scaling up to building-scale remains a challenge. To engender printability, a range of biopolymers, including psyllium husk,[9–12] chitosan,[13,14] guar gum,[15] xanthan gum,[16,17] locust bean gum,[11] corn starch,[11] cellulose,[14] agar,[18–21] and sodium alginate,[21,22] have been employed as rheology modifiers to improve extrudability, shape stability, and structural build-up.[23] Printable MBC pastes are typically formulated by mixing biopolymers with mycelium inoculum and fine substrate particles or fibers (length <1 mm). According to our MBC 3D printing literature review in Table S1, the overall height of printed structures rarely exceeds 10 cm, as the soft, moisture-rich, printed layers typically have weak interfacial bonding and lack a rapid solidification process to

[a] *Department of Architecture, Cornell University, Ithaca, NY 14853, USA. E-mail: mh2226@cornell.edu*
[b] *Sibley School of Mechanical and Aerospace Engineering, Cornell University, Ithaca, NY 14853, USA. E-mail: meredith.silberstein@cornell.edu*
[c] *Engineered Living Materials Institute, Cornell University, Ithaca, NY 14853, USA*

support subsequent layers. Solidification into a stable structure relies on mycelium colonization over several days to fuse the print layers during the post-printing period. As a result, current MBC 3D printing methods remain restricted to the centimeter scale.

We herein present the new concept of shooting as a scalable, geometry-flexible, and cost-efficient fabrication approach to advance MBC applications at the meter scale. Shooting methods are widely used in the sprayed concrete industry to pneumatically deposit materials onto arbitrarily oriented surfaces using high pressure air, enabling shape flexibility and rapid construction, such as surface coatings, shell structures, and iconic buildings.[24] Shootability is defined as the ability of cementitious materials to be deposited onto vertical surfaces without rebounding (requiring adhesion) or sagging (requiring cohesion).[25] Compared with extrusion-based 3D printing, high-pressure projection from shooting enables quick coverage of large areas and deposition flexibility.[26] To enable shootability, it is necessary to formulate initial mixtures with appropriate viscosity and flowability by incorporating additives as binders.[27] Even though 3D printing of MBCs has already employed biopolymers as cementitious binders, research on material processing to optimize biopolymer rheology is scarce, as most studies focus only on untreated mixture constituents and printing parameters (Table S1). The requirements for shootability may be more demanding than 3D printing due to the fabrication extending beyond the deposition of horizontal planar layers. We demonstrate that biopolymer modifications in MBCs are crucial to achieve the required bonding strength to keep the deposited material shape stable post shooting, prior to hyphal growth, thus enabling more flexible fabrication methods.

Biopolymers, including polysaccharides, proteins, and lipids, are extracted from renewable agro-resources, such as plants, animals, and microbes.[28] The use of natural biopolymers as gelling agents has received increased interest in industrial processes due to their rheological properties, non-toxicity, biocompatibility, and biodegradability in comparison to petrochemical-based synthetic polymers.[29] Specific parameters of physical, chemical, and biological modifications of biopolymers to achieve the gelling mechanism of sol (liquid)–gel (solid) transition have been extensively investigated for biodegradable films in packaging,[30] thickeners in the food industry,[31] stabilizers in soil reinforcement,[32] rheology controllers in the concrete industry,[33] adhesives in wood composites and the manufacturing industry,[34] and 3D-printable structures in the biomedical sector.[35] Physical modifications for controlling biopolymer rheology typically reduce the need for chemical reagents, are environmentally friendly, user friendly, and scalable. These modification approaches including blending and adjusting concentration, degree of dissolution, temperature, and pH.[36,37] Chemical modification of the rheological performance of gels can be achieved through chemical reactions, such as acylation, sulfation, hydroxylation, esterification, etherification, and graft copolymerization.[38,39] Biological modifications include enzymatic hydrolysis and enzymatic grafting.[40] The key to enhancing viscosity lies in effectively dissolving biopolymers, which promotes molecular entanglements to form a denser water-entrapped three-dimensional network.[41] Herein, a hypothesis is proposed that the viscosity and flowability of MBCs can be optimized for shooting by modifying biopolymers.

Here, we report the first study on engineering shootable MBCs, focusing on the innovations of tuning biopolymer treatment methods to support vertical deposition, and establishing shooting as a scalable, flexible fabrication approach for MBCs. To be able to shoot a mycelium mixture onto a vertical wall, the modified mixture must be adhesive enough to stick to the surface and cohesive enough to prevent crumbling after shooting. We selected psyllium husk powder as the mixture binder in this study due to its low cost and worldwide availability.[42] Psyllium husk is a plant-derived polysaccharide extracted from the seeds of plants in the *Plantago* genus, and is non-toxic and fully biodegradable.[43] Moreover, it exhibits strong gelling properties in an aqueous environment.[44] Psyllium husk has attracted significant attention as a gelling agent in 3D-printable mycelium material, as it is ideal for use in extrudable filaments and is biocompatible with mycelium growth.[15] However, previous studies typically directly mixed psyllium husk in its dry powder form with substrate–mycelium mixtures (Table S1). Compared to MBC 3D printing, we use similar material constituents but with larger substrate size (1–10 mm *vs.* 0.1–1 mm in printing) and introduce eco-friendly, additive-free modification methods for psyllium husk to maximize its effectiveness as the binder.

This study introduces a materials-centered experimental framework (Fig. 1) to investigate the interactions between biopolymers and key composite components: water (gelling), fiber (shooting), and mycelium (growth), thereby enabling the fabrication of shootable mycelium-bound composites. Systematic variation of psyllium husk gel preparation, including autoclaving parameters, concentrations, and dissolution time settings, revealed unique rheological properties as characterized and analyzed through flow rate tests, Fourier transform infrared (FTIR) spectroscopy, zeta potential, and rheometry. The shootability and shooting consistency of hemp–mycelium composites with psyllium husk were then evaluated as composites with varied concentration, retention (resting) time, mixing and addition methods. Finally, we assess mycelium growth and composite integrity through visual inspection, cross-sectional imaging, mass loss over growth time, and mechanical testing. By enabling vertical deposition and decoupling mycelium growth from rigid mold constraints, this approach broadens the design space for fabrication, and reduces labor and time constraints. Notably, these fully plant- and fungi-based compositions are biodegradable and compostable, eliminating waste generation and ensuring a closed-loop building lifecycle. The methodology introduced here offers a foundation for sprayable bio-based materials, particularly in adapting concrete-inspired spraying processes for scalable and sustainable building systems.

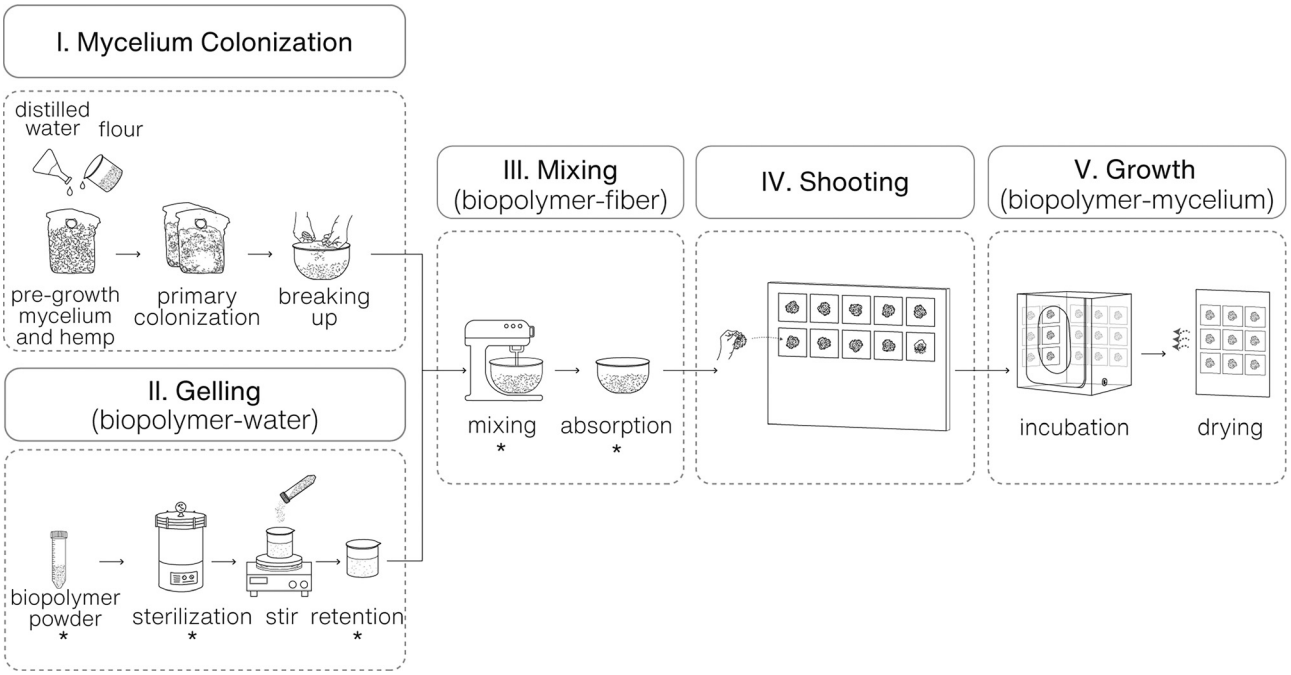

Fig. 1 Designed workflow for biopolymer modifications for shootable mycelium-bound composites. Incubation and drying can be conducted either in small containers or on a wall within a sterilized environment. Asterisk (*) indicates the material treatment parameters tested for shooting in this study.

2. Materials and methods

2.1. Materials

Dehydrated pre-inoculated hemp hurd–mycelium mixtures obtained from Ecovative Design (NY, USA) were selected for this study to ensure consistency. The Ecovative mixture is easy to use and relatively resilient to mold contamination.[10,14,45] Psyllium husk powder, used as the gelling agent, was purchased from Now Foods (IL, USA).

2.2. Preparation of psyllium husk dispersions

Before use, psyllium husk was autoclaved in dry powder form with a 50 mL centrifuge tube wrapped in aluminum foil at 121 °C for 15 minutes to remove contaminants. Thereafter, dispersions were prepared from autoclaved psyllium husk powder in varying concentrations of 2%, 2.5%, 3% and 3.5% by weight of distilled water. This range was selected based on preliminary tests that showed poor cohesion below this range and poor dispersibility above this range. The calculated amount of powder was dispersed in distilled water and magnetically stirred at 2000 rpm for 4 h at room temperature (25 °C). This stir rate was selected to maintain stable rotation of the stir bar and continuous mixing of the psyllium husk dispersion over the full 4-hour period. Afterwards, the dispersions were rested for 0 h, 6 h, 12 h, 18 h, or 24 h for each test. The prepared psyllium husk dispersions for further tests were labeled as P-*x*–*y*, where *x* represents the concentration and *y* is the retention (resting) time. For example, P-2.5–0 represents a sample with 2.5% psyllium husk by weight of water and 0 h of rest. This stage transformed the dry psyllium husk powder into dissolved psyllium husk dispersions.

2.3. Autoclaving psyllium husk and flow test

Viscosity and sterilization of psyllium husk were evaluated by assessing flow rate and contamination testing respectively, in order to determine the effective autoclaving parameters. Five psyllium husk samples were prepared: unautoclaved powder (control group), powders autoclaved for 15 min and 30 min, and dispersions (P-2.5–6; not mixed with hemp–mycelium mixture) autoclaved for 15 min and 30 min. For the flow test, powder samples were dissolved into dispersions after autoclaving, maintaining an equivalent concentration and retention time as autoclaved dispersion samples. Three replicates of all samples were tested after cooling back to room temperature (25 °C) using the International Dysphagia Diet Standardization Initiative (IDDSI) flow test.[46] Because some dispersions were too viscous to pass through a standard syringe tip, the IDDSI flow test was performed using a 10 mL syringe with the tip trimmed (barrel retained). For each sample, the volume of dispersion passing through the syringe over 10 seconds was measured and used to calculate the flow rate in mL s^{-1}. Subsequently, sterilization was assessed by transferring the samples to potato dextrose agar (PDA) plates and monitoring for contamination over 7 days.

2.4. FTIR spectroscopy

FTIR spectroscopy was performed using a Bruker Vertex FT-IR spectrometer (Bruker Corp., Billerica, MA) to identify changes in chemical composition in the psyllium husk powder samples with varied autoclaving times (0, 15, and 30 min). A spectral range of 4000 cm^{-1} to 500 cm^{-1} was selected to capture the peaks. Approximately 5 mg of powder sample was loaded into

the sample compartment to fully cover the attenuated total reflectance (ATR) crystal. The sample chamber was then vented with nitrogen before taking sample measurements following previous experimental methods.[47] The background (spectra with no sample loaded) was subtracted and spectra were analyzed using KnowItAll Informatics System 2023 (Wiley Science Solutions, Hoboken, NJ).

2.5. Zeta potential measurements

Zeta potential was measured using a Malvern Nano Zs Zetasizer (Malvern Panalytical, Malvern, U.K.) to understand colloidal stability of psyllium husk powder samples autoclaved for 0, 15, and 30 min. Solutions for three replicates were prepared in 15 mL tubes and given 30 minutes to equilibrate before being transferred to polystyrene or zeta potential folded capillary cuvettes for measurement. Samples were gently pipetted up and down to ensure a homogeneous sample distribution. Zeta potential was measured at a concentration of 0.1% with deionized water as the solvent as per manufacturer recommendations provided by Malvern Panalytical. The zetasizer calculates the zeta potential by finding the electrophoretic mobility and then applying the Henry equation.[48] Data was analyzed to determine if differences between groups were statistically significant. Two-tailed student *t*-tests were used to identify which differences were significant with a *p*-value of less than 0.05.

2.6. Rheological measurements

The rheological properties of psyllium husk dispersions with different concentrations and retention times were measured using a TA DHR3 rheometer (Texas Instruments, Dallas, TA), with a 40 mm diameter steel parallel plate and a gap of 1 mm. A 2 mL sample for each measurement was placed onto the Peltier plate. After loading the sample, any excess material was carefully removed from the edges to avoid artifacts, and the exposed sample edges were covered with a thin layer of low viscosity mineral oil to prevent water evaporation. All rheological measurements were carried out at 25 °C in triplicate.

First, oscillatory strain sweep tests were used to evaluate the viscoelastic properties of the formulations. The shear strain (γ) was swept from 0.1 to 100% maintaining an oscillation frequency of 0.5 Hz to determine the linear viscoelasticity region (LVR). Subsequently, frequency sweep tests ranging from 0.01 Hz to 5 Hz at a selected shear strain of 1% based on the LVR were performed to identify the phase transition of psyllium husk gels between solid-like elastic behavior and liquid-like viscous behavior. The viscoelastic response to applied shear strain was characterized by the loss modulus (G'') and the storage modulus (G'), to identify the phase transition (liquid-like or solid-like nature) of psyllium husk dispersions. Finally, the viscosity of psyllium husk gel as a function of shear rate was tested to evaluate the flow behavior of various formulations at different concentrations and retention times.

2.7. Preparation of mycelium-bound composites

The filter patch bag containing 450 g of dehydrated ingredients filled with pre-inoculated mycelium–hemp hurd mixtures was obtained from Ecovative. The mixture was then sieved to a particle size of 1–10 mm before use. To activate mycelium growth, the Ecovative mixture was rehydrated with 700 mL of distilled water and supplemented with 64 g of wheat flour as an additional nutrient source to accelerate growth. The bag was shaken manually until all ingredients were evenly distributed. Subsequently, the filter patch bag was placed in a climate-controlled grow tent equipped with air filtration, maintained at 65–70% relative humidity and 23–25 °C in a dark space. After three days of mycelium growth, the compacted content of the bag was broken up manually, facilitating homogenous mixtures and easier preparation. The mycelium mixture was used after five days.

2.8. Mixing psyllium husk–mycelium-enriched hemp fiber mixtures

The mixing experiment was implemented in two phases: (1) evaluation of the psyllium husk preparation method: (A) dry-powder and (B) pre-dissolution. (2) Adjustment of the mixing rate and mixing time.

Fig. 2 illustrates details of the dry-powder and pre-dissolution preparation methods, which were considered to find an effective preparation method for high shooting performance and facilitate understanding of the mechanisms of fiber–biopolymer interactions. As the control group, the dry-powder mix is the protocol commonly used in 3D printable mycelium composites: 550 g of mycelium mixture was put into the mixer, followed by 25 g of psyllium husk powder, and 1000 mL of water. The contents were fully mixed over the 90 s period at a low speed of 150 rpm using an electric stand mixer (Aucma Co., Ltd, 6.5QT Household Stand Mixer). For the pre-dissolution method, the prepared psyllium husk dispersion and mycelium mixture were combined as follows: P-2.5–12 dispersion was combined with the same amount of powder and water as used in the dry-powder method, and poured into the mixer while the hemp–mycelium mixture was gradually introduced.

In phase 2, the mixed material was prepared with P-2.5–12 dispersion and sampled at three different mixing times (30 s, 90 s, and 180 s) and mixing rates (150 rpm, 270 rpm, and 450 rpm) to evaluate the effect of mixing parameters on the workability of shooting. All experiments were performed in triplicate, with samples prepared in a mixer and subsequently shot onto the vertical surface at a 5-min interval. The optimal mixing parameters were determined based on the longest time span between the first and last successful shots, as observed in at least two shooting test sets for each mixing condition.

2.9. Shootability and shooting consistency measurements

Shootability defines the spray performance of concrete materials in the building industry, including the ability to allow a material to hold itself together (cohesion) and to stick to the shooting surface (adhesion).[25] According to the Standard Practice for Shotcrete, an acceptable rebound rate of sprayed material from the targeted surface is 5–20%.[49] Therefore,

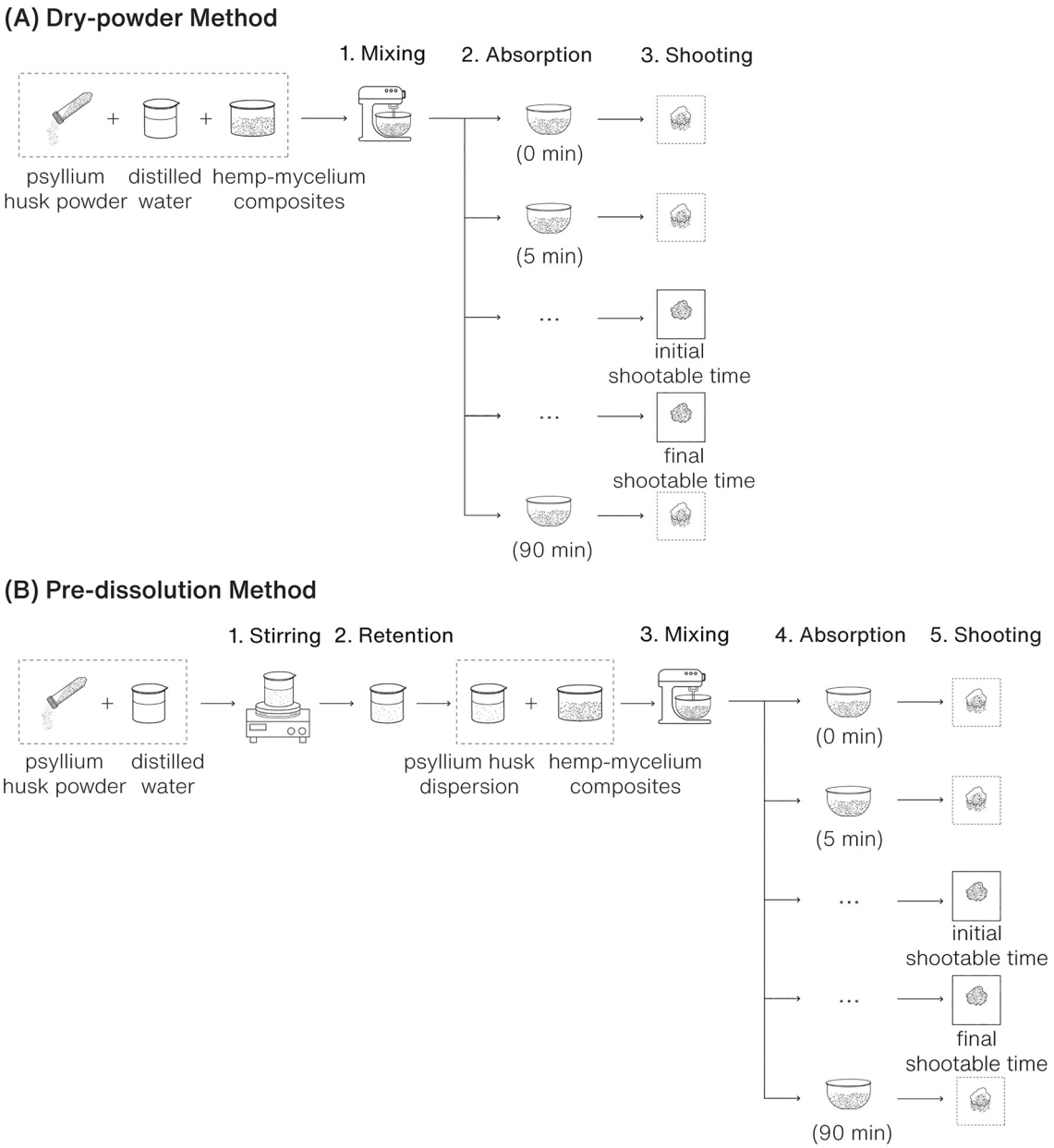

Fig. 2 Psyllium husk powder addition methods tested: (A) dry-powder and (B) pre-dissolution methods.

shootability in this study measuring above 80% was characterized as having good shooting performance.

To evaluate shootability, plywood panels were selected as vertical test surfaces according to the ASTM C1140/C1140M standard – "Preparing and Testing Specimens from Shotcrete Test Panels," since testing standards do not exist yet for shootable MBCs and ideal performance would be comparable to hydraulic cement mortar.[50] The procedure for quantifying the shootability of mycelium-bound mixes was as follows: (1) the tested sample ($\sim$0.8 g cm^{-3}) was extracted from the mixer using an 80 mL scoop; (2) the weight of each sample was measured before shooting; (3) calculated samples were manually shot onto separate sterilized vertical 15 $\times$ 15 cm plywood panels at a velocity of $\sim$2.4 m s^{-1}; (4) after the shape stabilized on the panels, the quantity of shot mixtures that fell from the vertical panel was weighed. Shootability, noted as S, was calculated using eqn (1).

$$S = \frac{(W_0 - W_1)}{W_0} \times 100\,[\%] \quad (1)$$

where: S = capacity of shootability [%], W_0 = initial sample weight before shooting [g], W_1 = the loss of sample weight after shooting [g].

The consistency of shootability was measured by recording the time between the first and last successful shots ($S > 80\%$) that occurred within the frame of absorption time. A successful shot is defined as a deposit adhering to the vertical panel with less than 20% of its mass falling off after impact and remaining

stable at least 5 hours. Absorption time begins after the mixing stage to measure the workable period during which mixes should ideally be used. Each sample was shot onto the panel at absorption intervals of 5 minutes until the latest shot mixture no longer adhered to the surface. The complete 90-min shootability test for each condition was repeated in triplicate. The duration of consistent high shootability was determined as it would influence the schedule of shooting operations in actual construction scenarios.

2.10. Mycelium growth assessment and mechanical testing

The shot samples were sealed in plastic bags and hung vertically in a climate-controlled growth tent at 23–25 °C with a relative humidity of 65–70%. A visual evaluation was performed on both the surface and inside of the samples for 7, 10, 14, or 21 days of growth. To more quantitatively study the effects of psyllium husk gel on mycelium growth and final material properties, mass loss over growth time, dry density, and response to uniaxial compression testing were measured by preparing specimens of hemp–mycelium composites with 2%, 2.5%, 3%, and 3.5% w/v of psyllium husk gels grown in plastic molds (3 × 3 × 3 cm) for 21 days. The original Ecovative composites without psyllium husk gel served as the control for this molded geometry. Considering oven drying is impractical for future large-scale construction applications, the specimens were then air-dried for four days to stop the mycelium

Fig. 3 Summary of mixture processing steps and experimental test set-ups from material preparation to final mycelium incubation: (a) autoclaving preparation of psyllium husk powder. (b) Stirring psyllium husk powder in distilled water. (c) Retention of psyllium husk gels for specific durations. (d) Rheometer with parallel plate geometry. (e) Original hemp–mycelium mixtures (five days after inoculation) with loose properties. (f) Mixing hemp–mycelium mixtures (five days after inoculation) with psyllium husk gel. (g) Extracting a single shooting sample from the mixing bowl and weighing it. (h) Shooting the sample onto the vertical surface. (i) Mycelium incubation in a vertical orientation. (j) and (k) Mycelium growth observation on the surface and across the cross-section. (l) Compression testing.

growth, until a constant mass was reached. Compression tests on the dried specimens were carried out on a Zwick-Roell (Zwick-Roell, Germany) Z010 system with a 10 kN load cell with a preload of 5 N at a strain rate of 0.01 s^{-1} to an engineering strain of 0.5, and then unloaded at the same strain rate back down to the preload; this was followed by a second cycle to the same maximum strain. Four compression experiments were conducted for each sample type. Engineering stress was obtained as the applied force divided by the initial cross-sectional area of a specimen. Engineering strain was determined by dividing the displacement of the crosshead by the initial specimen height. The dimensions of each sample were measured after drying and prior to mechanical testing, since shrinkage occurs during drying. The stress–strain curves were plotted to determine Young's modulus, calculated using the slope of the stress–strain curves over a strain range of 0.02–0.05, that was selected to avoid artifacts from sample surface imperfections and remain below yield for all samples, and the stress at the maximum applied strain of 0.5 during the first loading cycle. Fig. 3 shows a pictorial summary of the mixture processing steps and experimental test setups, from material preparation to final mycelium incubation.

3. Results and discussion

3.1. Autoclaving is needed for sterilization and influences viscosity

Unwanted microorganisms, such as bacteria and fungi, are a possible contamination source when fabricating MBCs.[51] Therefore, sterilizing the psyllium husk powder in an autoclave before mixing is recommended to reduce risk of contamination.[12] However, the autoclaving temperature and time were observed to alter the molecular structure of psyllium husk, thus influencing rheological properties of the prepared psyllium husk dispersions. Here, we determine the optimal protocols for sterilization time and the sterilized ingredient state, in order to find the right balance between high shootability and low contamination risk.

We compared the resulting flowability of psyllium husk autoclaved in its powder or dispersion form at 121 °C for either 15 min or 30 min (Table 1) using an IDDSI flow test. The flow rates of dispersions prepared with autoclaved dry powders showed a slight increase from 0.203 ± 0.009 mL s^{-1} to 0.291 ± 0.010 mL s^{-1} as the autoclaving time increased from 0 min to 30 min. The reverse trend was observed for the autoclaved dispersions, as the flow rate sharply decreased with increasing autoclaving time. The flow-resistant autoclaved dispersions resulted in poor shootability of hemp–mycelium mixtures. These overly stiff shooting composites failed to shoot onto the vertical panel and may be undesirable for future spray applications due to potential clogging or rebound issues.

The rheological changes of biopolymer gels are closely associated with modifications of interchain interactions, as well as orientation and deformation of molecules.[52] FTIR was used to analyze changes in chemical structure among the powder samples autoclaved for different times to understand the observed changes in viscosity (Fig. 4(a)). As expected, clear peaks are seen for the protein, lipid and polysaccharide regions, labeled based on literature on unpurified biofilms.[53] No clear shifts in peaks are observed among the 0, 15, and 30 minute samples. The autoclaved powders did exhibit increased peak intensity at 893 cm^{-1} due to the presence of β-glycosidic linkages.[54,55] Additionally, the loss of the shoulder at 856 cm^{-1}, associated with the α-linkage of furanose, with autoclaving suggests a reduction in arabinose branching.[54,55] These changes in polysaccharide structure with autoclaving likely decrease entanglements, corresponding to the increased flow rate.[56]

The zeta potential was measured to further understand the differences of gelling behavior from the autoclaving and to gain insight into the potential stability of the colloidal system. In Fig. 4(b), non-autoclaved powder samples were stable in solution, indicated by an absolute value greater than 20 mV, (−21.4 ± 2.0 mV). Powder samples after 15 min and 30 min autoclaving showed lower zeta potentials of −17.1 ± 2.7 mV and −17.3 ± 2.8 mV, respectively. Absolute zeta potential values below 20 mV indicate that they are less stable in solution and may be more likely to aggregate, which could account for their higher flow rate. It was reported that less aggregation provides molecules with more possibilities to interact and form a network to trap water and solubilized components, thereby enhancing viscosity.[37] The dependence of viscosity on colloidal stability observed in psyllium husk gels is attributed to the interaction between functional groups with water.[57–59] The change in zeta potential due to autoclaving indicates that a chemical reaction may have occurred that altered functional groups and changed the surface charge distribution, which is related to the zeta potential.[60–63]

We also verified that the psyllium husk powder used in the shootable mixtures was sterile after autoclaving. Fig. 4(c) shows the results of contamination tests for different autoclaving

Table 1 Flow rates of the psyllium husk gels with varied autoclaving parameters (n = 3). Significant differences between groups are indicated by superscript letters using two-tailed student t-tests, $p < 0.05$. Groups sharing a letter are not significantly different

No.	Autoclaved psyllium husk state	Autoclaving time (min)	Concentration (% w/v)	Retention time (h)	Flow rate (mL s^{-1})
P-0	N/A	0	2.5	6	0.203 ± 0.009[c]
P-P-15	Powder	15	2.5	6	0.229 ± 0.006[b]
P-P-30	Powder	30	2.5	6	0.291 ± 0.010[a]
P-D-15	Dispersion	15	2.5	6	0.077 ± 0.003[d]
P-D-30	Dispersion	30	2.5	6	0.023 ± 0.000[e]

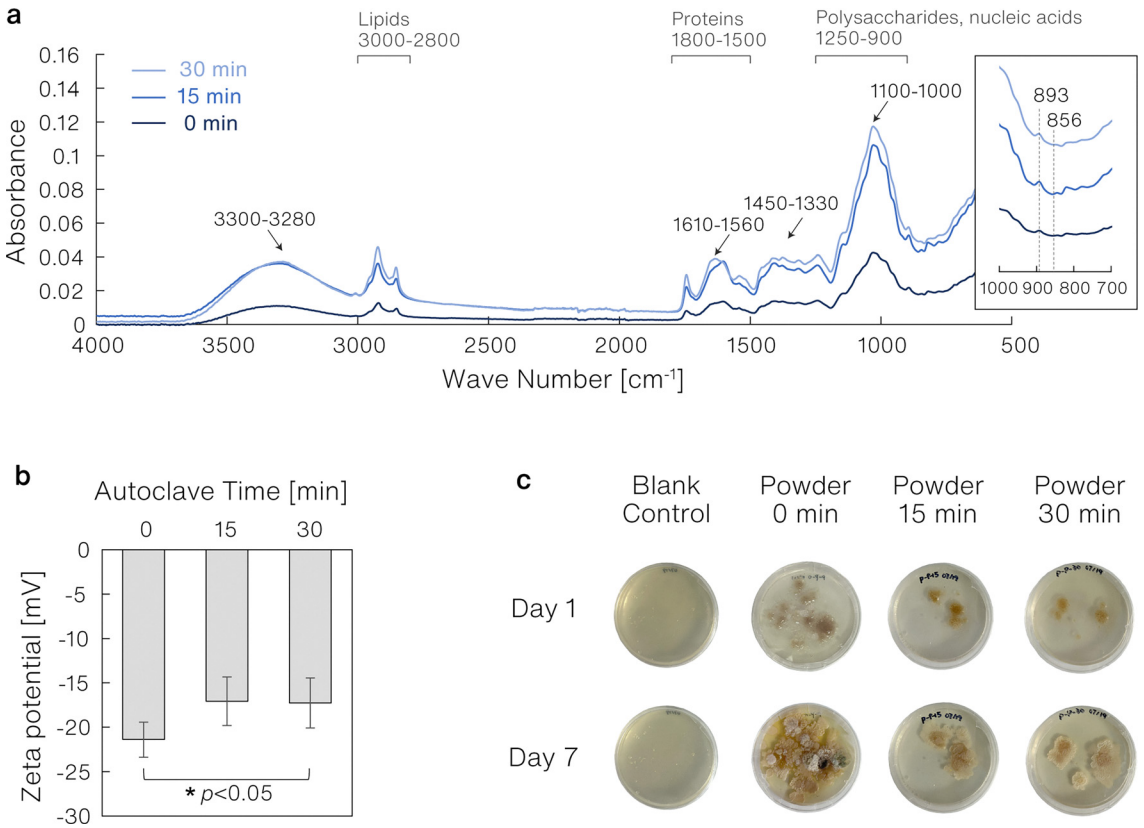

Fig. 4 (a) Results from FTIR tests with psyllium husk powders autoclaved for different times. The spectra show the emergence of a small peak and shoulder between 1000–800 cm^{-1} shown in the inset. (b) Zeta potential values for psyllium husk powders autoclaved for different times (n = 3); p-values are indicated by asterisks, *$p < 0.05$. (c) Contamination testing of psyllium husk powder at different autoclaving times on potato dextrose agar (PDA) media.

times. After 7 days on potato dextrose agar (PDA), the psyllium husk powder that was not autoclaved showed clear signs of contamination. Single colonies of bacterial spores were observed from the 15-min and 30-min autoclaved psyllium husk powders, but further visual observations did not indicate the bacterial growth compromising the mycelium growth. Overall, psyllium husk powders autoclaved for 15 min exhibited the optimal viscous features of a gel and effective sterilization for shootable mycelium mixtures.

3.2. Retention time and concentration of psyllium husk gel affect shootability

Shootability (S) of hemp–mycelium composites with psyllium husk gel addition was evaluated as a function of absorption time to determine the optimal biopolymer formulations for shootable hemp–mycelium mixtures. Absorption time is the duration that mycelium-enriched fibers and psyllium husk gel remain together after mixing and before shooting, throughout which the duration of shootability was evaluated. Evaluating the processable time period of shootability is particularly beneficial for future construction applications. The results of S and its consistency across different concentrations of psyllium husk dispersions with retention times of (resting for) 0, 6, 12, 18, and 24 h are shown in Fig. 5(a) and Table S2, revealing a non-monotonic relationship between S and both psyllium concentration and retention time. Optimal formulations—P-2.5–18, P-3.0–12, P-3.0–18, and P-3.5–12—exhibited stabilized high S over an absorption time range of 40–50 min. Notably, P-3.0–12 exhibited the highest S with extended total shootable time (>50 min, Fig. 5(b)). In contrast, retention times of 0, 6, and 24 h resulted in unstable S regardless of absorption time. Short retention times may cause insufficient psyllium husk dissolution, instead remaining strongly intramolecularly connected. 24-h retention time likely led to excessive dissolution, limiting the bonding behavior of mixes due to molecular degradation caused by the breakdown of covalent bonds and separation of monomers.[64,65] The retention time required for consistent S decreased from 18 h to 12 h as psyllium husk concentration increased from 2% w/v to 3.5% w/v. Mixes with 2% w/v psyllium husk gel demonstrated unstable S for all retention times, as shown by shooting samples breaking and splashing when colliding with the surface (Fig. 5(c)). 3.5% w/v of psyllium husk gel produced stiffer mixed samples with a tendency to rebound from the surface (Fig. 5(d)).

We conducted rheological measurements on psyllium husk dispersions at different concentrations and retention times corresponding to those used in the hemp–mycelium composites to better understand the shooting performance observed

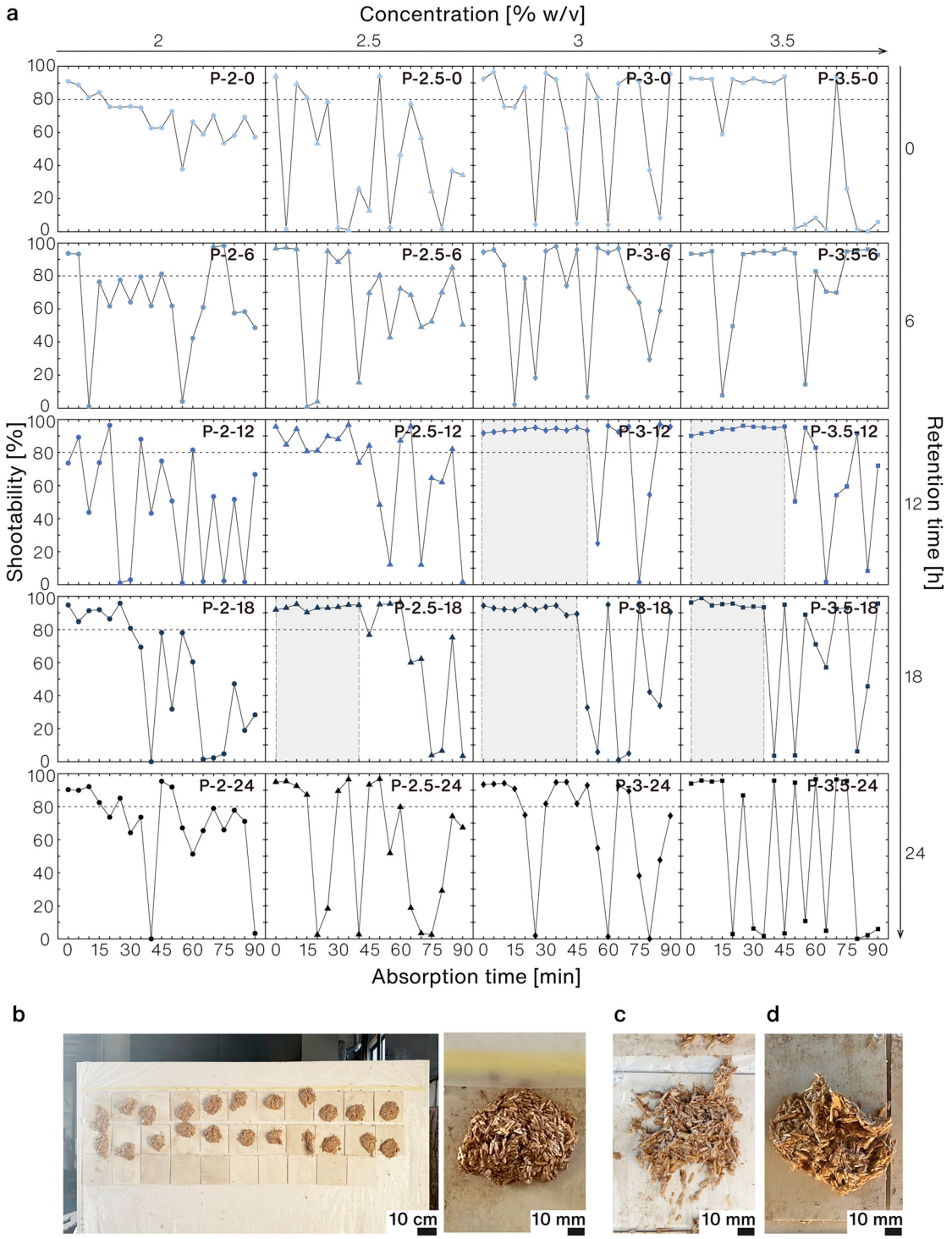

Fig. 5 (a) Representative shootability and shooting consistency measurements for various retention times and concentrations of psyllium husk dispersions. Replicate results (n = 3) for each condition are presented in Table S2. Shades in grey indicated the optimal range of shootability. (b) High cohesion and adhesion of mycelium mixtures containing psyllium husk dispersions of P-3–12. (c) Poor cohesion was observed in mixes with 2% psyllium husk gel. (d) Sagging and debonding was noted in the shooting sample with 3.5% w/v of psyllium husk gel, indicating part of the sample rebounded from the surface rather than adhering.

above. Specifically, we measured the storage (G') and loss (G'') moduli as functions of frequency and viscosity as a function of shear rate. Fig. 6(a)–(d) presents the storage and loss moduli of gel samples for a range of concentrations (2, 2.5, 3 and 3.5% w/v) and retention times of 0, 12, and 24 h. The psyllium husk dispersions at all concentrations behave in a predominantly solid-like gel manner with G' greater than G''. The only exceptions to this solid-like nature are the 3% and 3.5% w/v

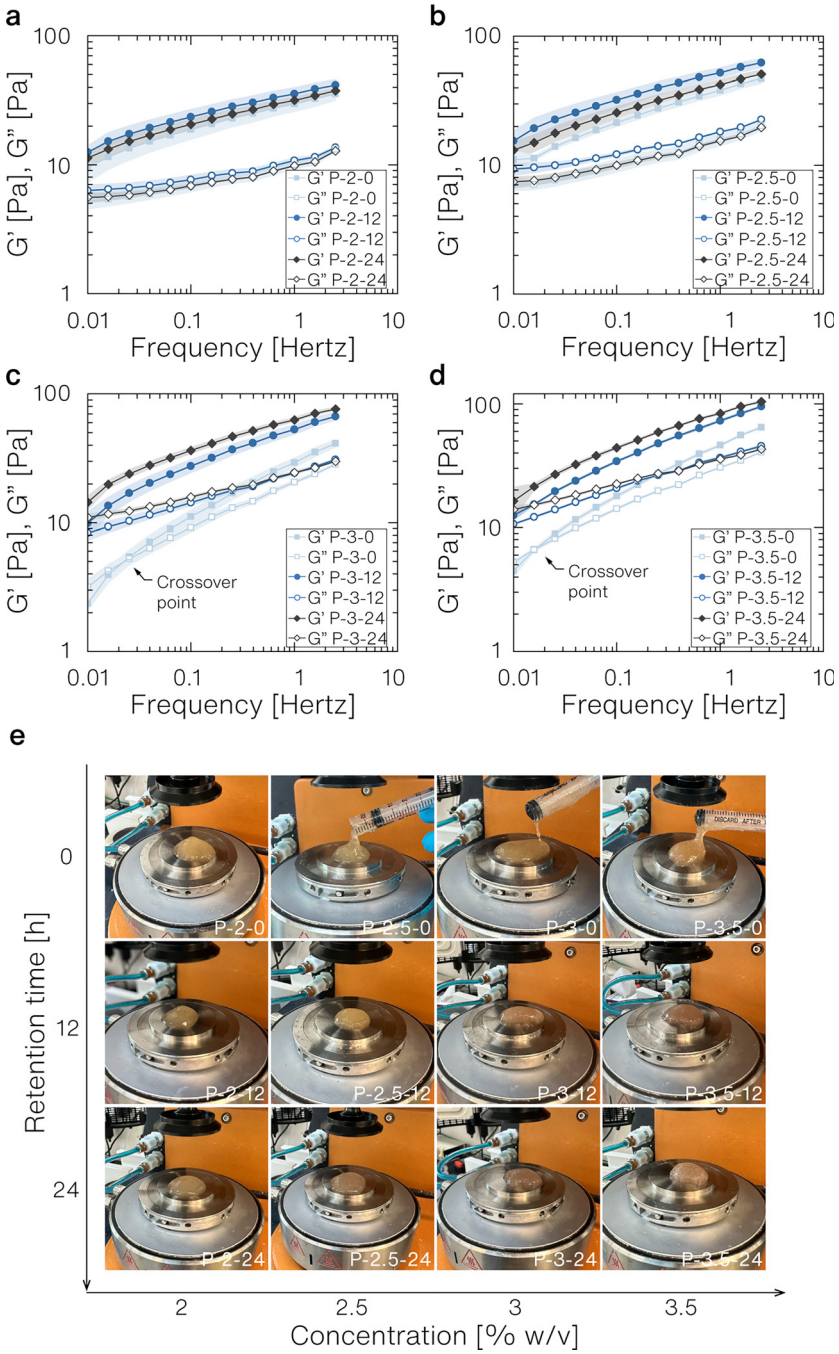

Fig. 6 Rheological properties of psyllium husk gels. (a)–(d) Rheological measurement of G' and G'' of psyllium husk gels at different concentrations and retention times (n = 3). (e) Droplets of psyllium husk gel for varied concentrations and retention times. Bubbles were observed in P-3–24 and P-3.5–24.

samples at low frequencies. Additionally, rate dependence is apparent for all formulations, as both moduli increase with increasing frequency. Furthermore, it was found that retention time had a substantial influence on the elastic properties of psyllium husk gels, especially at the higher concentrations of psyllium husk (3% and 3.5% w/v), where the longer retention time resulted in a clearly stiffer gel. Stable bubbles were formed in 3% and 3.5% w/v psyllium husk gels at 24-h retention time (Fig. 6(e)). Ren *et al.* (2020) ascribed the bubbles they observed in the heated psyllium husk dispersion to gel structure transitions, where concentrated suspension of packed gel particles are hydrated and swelled to form junction zones, with fibrous structures linked by cloudy areas.[55]

The relevance of these rheological properties for shootability can be understood through the viscoelastic droplet impact dynamics literature (Table S5).[66] Given our shooting parameters, we are operating in the low Reynolds (Re) number regime (Re $<$ 100), where Re gives the ratio of inertial to

viscous forces. The psyllium husk gels need to hold the hemp hurd fibers within the composite together as the material impacts the wall, allowing them to deform and dissipate sufficient energy to prevent rebounding from the surface. For shear thinning viscoelastic fluids, as we have here for all treatments (Fig. S2 and Table S4), the normalized contact line width (maximum diameter over initial diameter) and contact time should decrease with increases in either effective viscosity or elastic stiffness.[67] The tendency to rebound is best characterized by the Ohnesorge number (Oh), conceptualizing the drop as a linear mass-spring-dashpot system, where Oh $>$ 2 will suppress rebounding. Oh is the ratio of the square root of the Weber number (We) to Re, where We is itself the ratio of inertia to surface tension. Oh is linearly proportional to the effective viscosity, and therefore greater viscosity (*e.g.* energy dissipation) will suppress rebound for a set surface tension and droplet size.[68] These conflicting trends in expected performance with material property changes lead to non-trivial viscoelasticity design rules and likely non-monotonic shootability performance trends of the gel–hemp fiber composite, with psyllium husk gel rheological properties. Additionally, it is essential that the psyllium husk gel is not liquid-like at low frequencies (post impact and prior to significant drying or mycelium growth) or the composite will fall apart. P-3–0 and P-3.5–0 can therefore be ruled out as viable gels to use because G'' exceeds G' at low frequency. Finally, since the wall is vertical rather than horizontal as in most droplet dynamics literature, it is also important for the psyllium husk gel to provide adhesion to the wall. Given that elasticity here is based on non-covalent interactions (entanglements, as well as hydrogen and ionic bonds), we expect hydrated state adhesion to scale with G' accompanied by sufficient G''.[69–71] From this perspective we expect the higher concentrations to have better adhesion and therefore shootability performance for a given retention time, which is observed to be true for the most part. Gels used to support extrusion-based 3D printing of MBCs exhibited a G' (10^3–10^4 Pa) and a relatively low G'' (10^2–10^3 Pa) at low frequencies to prevent filament sagging.[19] As expected given the distinct deposition modes, these dynamic moduli ranges are quite different from the gels used to support our shooting samples, which displayed a much lower G' (10^1–10^2 Pa) with a closely matched G''.

3.3. Shootability is additionally influenced by mixing parameters

3.3.1. Addition method. The results of shootability and shooting consistency of mixtures of psyllium husk powder/dispersion with mycelium–hemp fibers prepared with different methods (dry-mix and pre-dissolution) at the equivalent psyllium husk concentration (2.5% w/v), retention time (12 h), and mixer parameters (90 s, 150 rpm) are shown in Fig. 7(a). It appeared that S was significantly higher when the psyllium husk powder was pre-dissolved in water than with the dry addition. The dry-mix method exhibited a low S value, under 30%, during the absorption time between 0–40 min and low consistency of bonding between 45–65 min. Conversely, the samples prepared by the pre-dissolution method showed a high S value, above 80%, with a prolonged absorption time from 0 min to 45 min. This suggests that the weak bonding performance of the dry-mix method is due to the lower amount of dissolved psyllium husk powder acting as a binder. Gonzalez-Avina *et al.* indicated that with insufficient dissolution, biopolymers aggregate and have limited effectiveness, as they are formed by strong intermolecular associations due to the abundance of hydroxyl groups in the dense internal network of biopolymers.[33] It was reported that sufficient dissolution enhances the amount of available biopolymers to increase the rheological properties, in the case of cement admixtures.[41] Several studies on wood adhesives showed that effective hydration of biopolymers improved internal bond strength.[72]

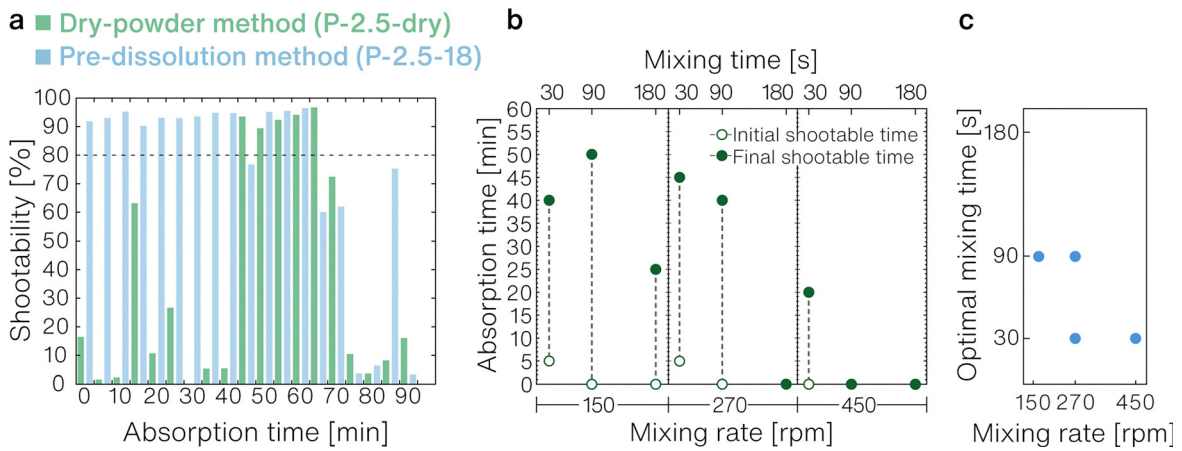

Fig. 7 (a) Representative results of shootability and shooting consistency from two addition methods for mixing psyllium husk with mycelium mixtures: (I) dry-powder method and (II) pre-dissolution method. Replicate measurements (n = 3) are presented in Table S2. (b) Initial and final shootable times of hemp–mycelium composites with psyllium husk gel addition (P-2.5–12) at different mixing rates and mixing times for pre-dissolution method. The shootable time is determined by the shootability being above 80% in at least two sets of the shootability test (n = 3) for each mixing condition. Replicate test data are provided in Table S3. (c) Each mixing rate has an optimal mixing time that yields the optimal shootable time range. Mixing for 30 s and 90 s at the middle rate (270 rpm) showed the same shootable time range.

Similarly, in this experiment, the mechanism of biopolymer–fiber interaction to achieve high shootability of shootable mixes is also influenced by the effective degree of biopolymer dispersion, dissolution, and swelling.

3.3.2. Mixing rate and mixing time. The effect of mixing rate and mixing time of hemp–mycelium mixtures with pre-dissolved psyllium husk gel on the initial and final shootable time is shown in Fig. 7(b) and (c). The valid shootable time is again evaluated by the shootability being above 80%. The results indicate that mixing rate and mixing time have a direct effect on the shootability and consistency of the shootable mixtures over a prolonged duration. The shootable time increases over the range of 30–90 s mixing time at the mixing rate of 150 rpm, which might result from the gradual homogenization of the mix. The longest shootable time was obtained at a 90 s mixing time and 150 rpm mixing rate. When the mixing time was increased to 180 s at a varied mixing rate range, water began to bleed from the mixes, resulting in unstable shootability. The final shootable time showed a gradual decrease with the increase in the mixing rate (Table S3), possibly due to a decrease in viscosity of the overall mixture, which we observed to become more watery and less sticky during the experiment (Fig. S3). The decrease in shootable time, caused by a higher mixing rate and prolonged mixing time, might be related to the destroyed intermolecular bonds in the gel network and the realignment of gel chains parallel to the flow direction by continual mixing or a higher shear rate, leading to lower flow resistance.[73] Decreased viscous and stabilizing properties, caused by polymer degradation after high-pressure homogenization, were also observed for other polysaccharides, such as methylcellulose, alginate, κ-carrageenan, and xanthan gum.[74,75]

3.4. Psyllium husk decreases growth rate but increases final composite density and stiffness

The psyllium husk dispersion functioned as a binder to consolidate the dry fiber-based mycelium mixture on vertical surfaces during shooting. After shooting, mycelium colonized the vertical mixtures, converting the material conditions from soft to hard. Following 21 days of growth, Fig. 8(a) and (b) shows the influence of psyllium husk concentrations of 2%, 2.5%, 3%, and 3.5% w/v on the mycelium growth rate and growth density both on the surface and in the cross-section with the same ratio of psyllium husk gel to hemp hurd fibers. Based on the visual assessment, the growth rate of mycelium on the surface was not substantially impacted by the concentrations of psyllium husk gel. This behavior is different from the faster surface growth with increased biopolymer concentration observed from mycelium growth on bamboo fibers with chitosan serving as the binder.[13] Interestingly, observations inside the samples revealed that higher concentration (3.5% w/v) of psyllium husk gel caused greater delays in mycelium growth, where the mycelial network was sparsely distributed after 14 days, while lower concentrations of 2% w/v resulted in denser mycelium branching integrated with hemp fibers inside the mixes (Fig. 8(b)).

To better quantify the dependence of the final composite on concentration of psyllium husk gel, equivalent samples were cultured within a cubic mold of similar overall volume. The weight of the samples was analyzed in terms of mass loss throughout the 21-day growth period; the Ecovative MBCs with no psyllium husk gel is included as a reference (Fig. 8(c) and (d)). All of the hemp–mycelium composites with psyllium husk gel start at a similar mass to each other that is more than twice that of the Ecovative MBCs. The mixes with 2% w/v of psyllium husk gel showed marked mass reduction on day 4 due to water bleeding from the gel, leading to drier substrates, whereas 3.5% w/v retained moisture the longest, as indicated by the smallest mass change over the growth period, and consistent with the visual observations of the least mycelium growth in the shot samples. The density for dry samples was also measured to further support that the higher mass loss at lower psyllium husk concentration corresponded to the increased mycelium growth, driven by the fungal degradation of lignocellulosic fibers.[76] In Table 2, the dry density of 203.6 ± 6.9 kg m^{-3} at 3.5% w/v indicated less fiber decay compared with 159.8 ± 10.9 kg m^{-3} and 175.9 ± 6.8 kg m^{-3} in Ecovative and 2% w/v samples, respectively. These findings suggest that mycelium growth started when the water within psyllium husk gel evaporated and fibers became less humid, which could be explained by the high water-holding capacity of psyllium husk gel.[77,78] The gel with higher viscosity may fill air voids inside the mix and bind fibers tightly, inhibiting sufficient oxygen permeation and thereby slowing the mycelium growth.[3] Our results suggest that the commonly reported issue of scarce mycelial growth in the core of 3D-printed MBCs may be due to excessive moisture (higher gel concentrations, 5–10% w/v *vs.* 2–3.5% in our study) and the absence of air voids (smaller substrate sizes, 0.15–1 mm *vs.* 1–10 mm in ours) (Table S1).

Despite the reduced mycelium colonization in composites with higher psyllium husk gel concentrations, the mechanical properties of the dried samples increased as the psyllium husk content increased (Fig. 8(e)–(g)). The shape of the hemp–mycelium composite stress–strain curves are somewhat different with the addition of psyllium husk gel, with the initial stiff linear regime followed by a rollover to a lower slope around a strain of 0.1, whereas the Ecovative composite remains roughly linear. All of the formulations exhibit a mix of plasticity and damage by the maximum imposed strain of 0.5, as evidenced by crackling sounds heard during testing, large residual strain, and the reduced modulus upon reloading. All hemp–mycelium composites containing psyllium husk gels showed an increase in Young's modulus compared to the Ecovative composite, indicating that psyllium husk gel improves the stiffness of conventional mycelium composites (Fig. 8(f)). Interestingly, the peak engineering stress of the loading cycle for all of the composites was similar, with only the 3.5% w/v samples showing a statistically significant increase; we suspect this is due to the relatively high dry density rather than a direct binding effect of the gel or mycelium growth. The reported values for Ecovative in literature are 30–122 kg m^{-3} for dry density, 0.04–1.03 MPa for compressive strength, and 0.6–2 MPa for

compressive modulus.[79–81] In previous 3D-printed MBC studies (where gel concentration was not varied), reports on stiffness of dried samples before and after colonization vary extensively. Shen *et al.* found that colonized cellulose–chitosan–coffee ground composites had over a 2.5-fold decrease in compressive modulus compared to uncolonized samples (38.3 *vs.* 98.7 MPa), whereas Luo *et al.* observed a lower modulus in uncolonized xanthan–coffee ground samples than in colonized samples

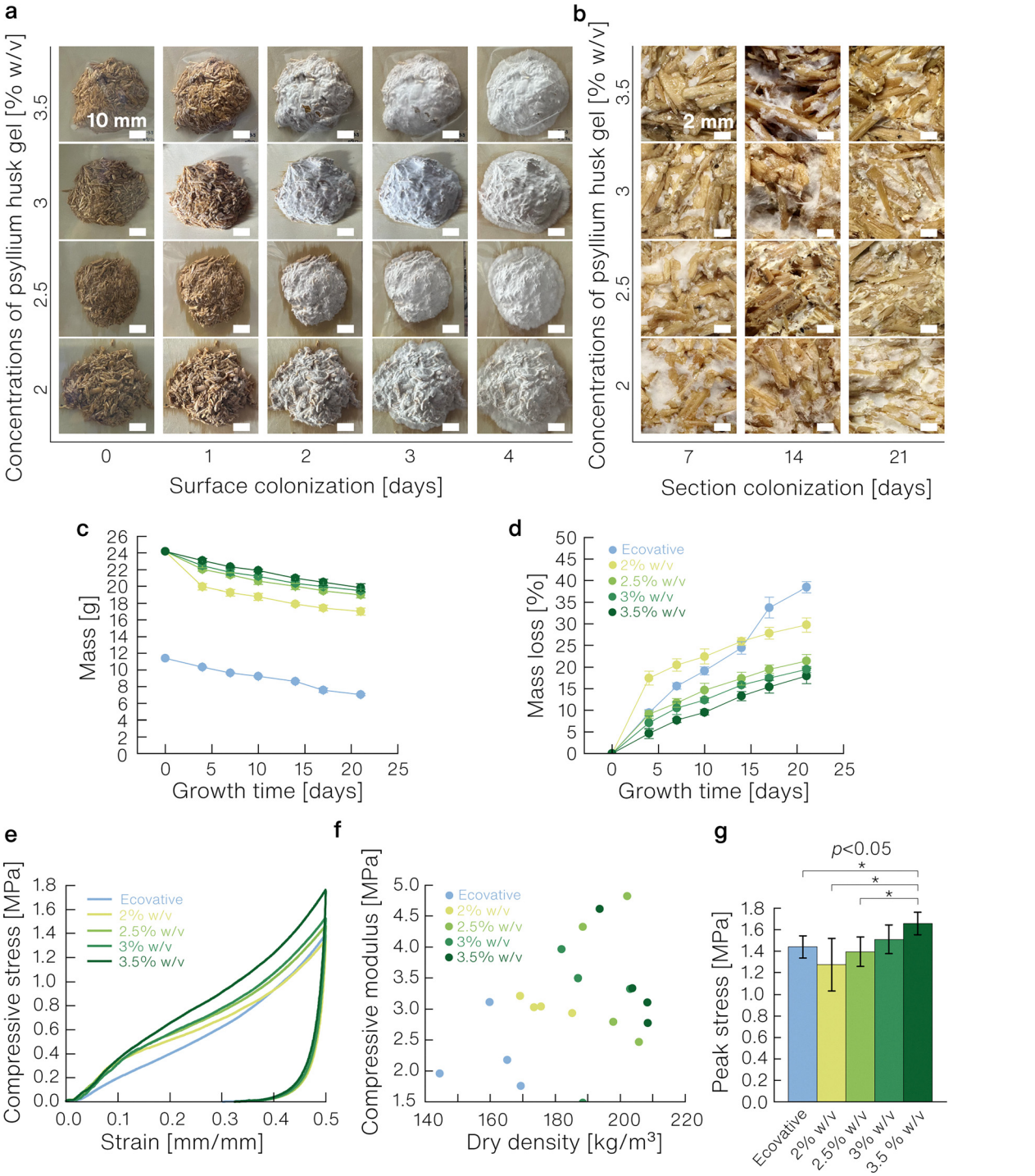

Fig. 8 (a) and (b) Mycelium growth on vertical plywood panels. Images of mycelium colonization on the surface (a) and throughout the cross-section (b) of shot samples containing psyllium husk concentrations of 2%, 2.5%, 3%, and 3.5% w/v at different growth days. (c)–(g) Mycelium growth within cubic molds. (c) Mass decrease of hemp–mycelium composites with and without psyllium husk gel as a function of growth time (n = 5). (d) Percentage mass loss as a function of mycelium growth time (n = 5). (e) Representative stress–strain curves, over one load–unload cycle, of the dried composites with different psyllium husk content (n = 4). (f) Young's modulus as a function of dry density (n = 4). (g) Compressive stress at the maximum applied strain value of 0.5 from the first loading cycle (n = 4); p-values are indicated by stars, *$p < 0.05$.

Table 2 Summary of physical and mechanical properties of hemp–mycelium composites with and without psyllium husk gel after 21 days of growth (n = 4 or 5). Significant differences between groups are indicated by superscript letters using two-tailed student t-tests, $p < 0.05$. Groups sharing a letter are not significantly different

Group	Mass loss during growth (%)	Mass before drying (g)	Mass after drying (g)	Dry density (kg m^{-3})	Young's modulus (MPa)	Compressive strength (MPa)
Ecovative	38.47 ± 1.26^{a}	7.02 ± 0.13^{d}	4.07 ± 0.25^{b}	159.77 ± 10.90^{c}	2.25 ± 0.60^{c}	1.44 ± 0.10^{b}
2% w/v	29.74 ± 1.66^{b}	17.02 ± 0.42^{c}	4.30 ± 0.26^{b}	175.92 ± 6.78^{b}	3.05 ± 0.11^{b}	1.28 ± 0.24^{b}
2.5% w/v	21.42 ± 1.52^{c}	19.02 ± 0.35^{b}	4.80 ± 0.16^{a}	198.58 ± 7.44^{a}	3.60 ± 1.15^{a,b,c}	1.40 ± 0.14^{b}
3% w/v	19.45 ± 0.72^{d}	19.48 ± 0.47^{a}	4.73 ± 0.16^{a}	190.13 ± 9.09^{a}	3.59 ± 0.33^{a}	1.51 ± 0.13^{a,b}
3.5% w/v	17.95 ± 1.80^{d}	19.86 ± 0.47^{a}	5.04 ± 0.31^{a}	203.61 ± 6.94^{a}	3.46 ± 0.81^{a}	1.66 ± 0.11^{a}

(15.2 *vs.* 17.08 MPa).[14,17] Future studies such as SEM imaging and fiber–matrix adhesion testing are needed to clarify the bonding interaction mechanisms of mycelial hybrid growth within biopolymer gel-infused matrices.

3.5. Challenges and prospects of spraying living MBCs at the building scale

The shootability of MBCs offers potential to create functional applications with freeform designs and unprecedented fabrication speed at building scale. Using formulated shootable MBC mixtures, we constructed a meter-scale freeform object (1.0 × 0.7 × 0.02 m) as a proof-of-concept for spray-based, *in situ* construction. This object is self-supporting after being grown and drying over 20 days (7-min spray, 10-day growth, and 10-day air dry) (Fig. 9(a)), similar to the curing time of 28 days for sprayed cement mortar (composed of cement, sand, and water). Our initial trials with conventional cement mortar spray hardware showed that shootable MBCs failed to flow through the nozzle, as they are relatively lightweight and viscous compared to cement mortar. We thus refined the spray gun into a cylinder form with dual pressure ports, allowing for synchronized air and mechanical pressure to drive material through the nozzle (Fig. 9(b)). Our cumulative thickness tests *via* single-spot spraying yielded a maximum deposition thickness of 40 mm with a conical shape (Fig. 9(c)), whereas sprayed cement mortar exhibited uniform cylindrical stacking with a thickness of 50 mm.[26] Shifting the shooting concept to practical construction thus requires future research on customizing spray hardware systems tailored to shootable MBCs.

Although MBCs have lower durability and weaker mechanical strength than cement mortar (Fig. 9(d)), the fully bio-based, low-energy manufacturing is more eco-friendly. Unlike cement mortar, which is produced through energy-intensive chemical reactions, the formation of mycelium-bound building materials

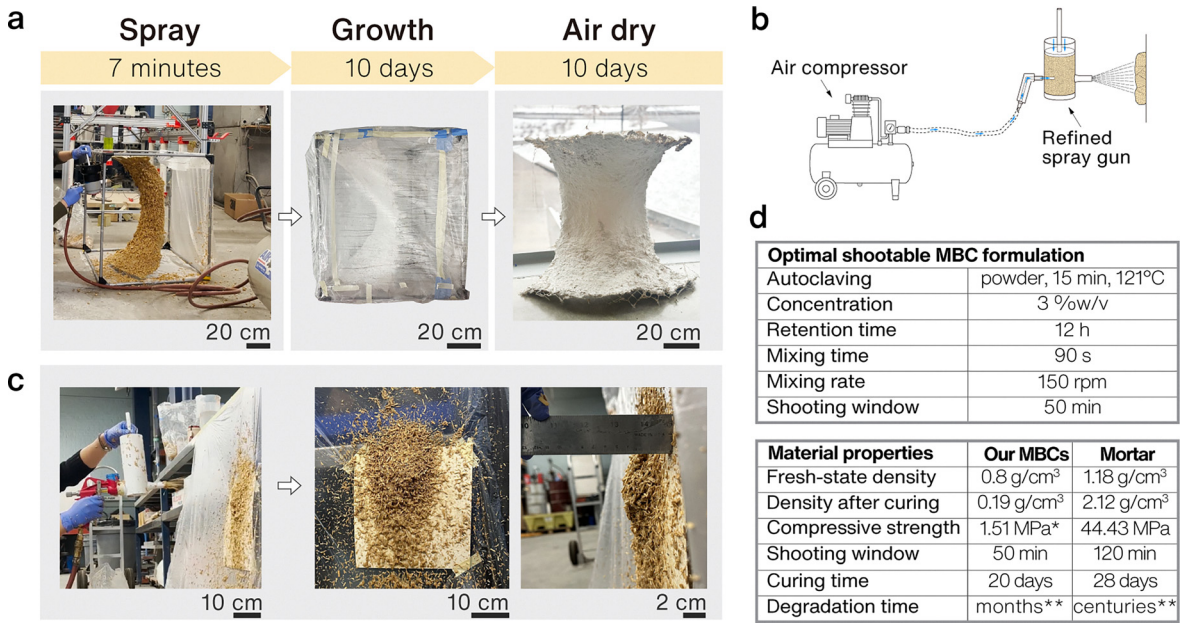

d

Optimal shootable MBC formulation	
Autoclaving	powder, 15 min, 121°C
Concentration	3 %w/v
Retention time	12 h
Mixing time	90 s
Mixing rate	150 rpm
Shooting window	50 min

Material properties	Our MBCs	Mortar
Fresh-state density	0.8 g/cm^3	1.18 g/cm^3
Density after curing	0.19 g/cm^3	2.12 g/cm^3
Compressive strength	1.51 MPa*	44.43 MPa
Shooting window	50 min	120 min
Curing time	20 days	28 days
Degradation time	months**	centuries**

Fig. 9 (a) Construction process of a meter-scale freeform object (1.0 × 0.7 × 0.02 m) as a proof-of-concept. Note: the growth image is rotated 90 degrees for consistent visualization. After two days of growth, the sample was placed horizontally because the tensioned flexible fabric (deposition base) tended to deform under the weight of the mixtures. (b) Refined spray hardware for shootable MBC formulations. (c) Cumulative deposition thickness tests *via* single-spot spraying. (d) Table summary of optimal shootable MBC parameters; side-by-side material property comparison between shootable MBCs and sprayed mortar. Information on sprayed mortar is reported by Liu *et al.* and Skripkiunas *et al.*[26,83] Note: * the compressive strength of our MBCs was tested after 21-day growth referring to the stress at a strain level of 0.5, rather than the maximum stress prior to failure. ** Degradation time of MBCs is reported by Van Wylick *et al.*, indicating a 43% mass loss of the composites after 16 weeks in soil,[84] which is likely a worst case estimate, while a comparable mass loss of mortar has not been reported.

is an innate biological binding process that harnesses the living nature of mycelium self-growth. Further, the revivability of inert mycelium-bound materials presents a promising avenue for addressing damage in building applications through their self-repair capacity.[82]

Shootability of MBCs can be exploited within specific construction scenarios. One envisioned application is the creation of continuous, seamless interior insulation layers that conform to curved or irregular building envelopes, thereby reducing heat losses through interfacial gaps and providing a sustainable alternative to conventional synthetic insulation materials, such as expanded polystyrene and polyurethane. Spray techniques also support rapid *in situ* fabrication, substantially reducing reliance on intensive labor and transportation of prefabricated molds. Further, this deposition approach is well suited for production of emergency disaster shelters since it can be conducted in non-sterile environments and has simple incubation requirements. Although MBCs inherently exhibit relatively low mechanical strength, the flexibility of spray techniques enables buildup of structural mass on preinstalled internal reinforcements.

4. Conclusions

This study highlights the influence of sustainable biopolymer modifications on rheological properties to help enhance the shooting performance of MBCs. We investigated psyllium husk as a rheological modifier for hemp–mycelium composites. Our approach constitutes a step change in the fabrication of MBCs as a shootable material that expands the application potential for automated, scalable, and flexible manufacturing processes. Shootable MBC formulations were developed, exhibiting high shootability (material loss $<10\%$) and consistent shooting time (greater than 50 min), which allowed for stable deposition on vertical surfaces. Effective dissolution was found to be critical for obtaining suitable rheological stiffness and viscosity of psyllium husk gel, ensuring that shootable MBCs maintain integrity when shot onto the surface and adhere strongly to the wall without sagging. Hence, the study reveals that psyllium husk processing parameters (*e.g.*, temperature and autoclaving time, concentration, retention time, mixing time, mixing rate, and addition method) can only vary within a narrow range for optimal shootability over a continuous duration. Although higher psyllium husk concentrations were found to slow mycelium growth inside the composite, the composition ultimately yielded increased compressive stiffness, compared with mycelium composites without psyllium husk gel. The shootable MBCs could promote high efficiency of large-scale construction, paving the way for further research on spraying techniques that reduce labor and overcome geometry limitations by functionally replicating the automated shotcrete fabrication process.

Author contributions

Conceptualization, X. B. B.; data curation, X. B. B., E. W. v. W., M. N. S.; formal analysis, X. B. B., E. W. v. W.; writing – original draft, X. B. B.; writing – review and editing, E. W. v. W., M. N. S., M. H. W.; visualization, X. B. B.; supervision, M. N. S., M. H. W.; project administration, M. N. S., M. H. W.; funding acquisition, X. B. B., M. N. S., M. H. W.; all authors have read and agreed to the published version of the manuscript.

Conflicts of interest

There are no conflicts to declare.

Data availability

Data for this article are available at Zenodo at **https://doi.org/10.5281/zenodo.15685571**.

Supplementary information is available. See DOI: **https://doi.org/10.1039/d5ma00656b**.

Acknowledgements

The authors would like to thank Cornell University's Regenerative Architecture Lab (ReAL), Circular Construction Lab (CCL), and James Strait for sharing their equipment and space to conduct the experiment. E. W. v. W. was supported by an NSERC CGS-D scholarship. The authors thank the Cornell Department of Architecture (thesis funding) and the Cornell Atkinson Center for Sustainability (Academic Venture Fund (AVF) MycoBuilt) for their financial support. This work was supported and performed in part at the Engineered Living Materials Institute (ELMI) at Cornell University. This work was performed in part at the Cornell NanoScale Facility, a member of the National Nanotechnology Coordinated Infrastructure (NNCI), which is supported by the National Science Foundation (grant NNCI-2025233). The work made use of the Cornell Center for Materials Research shared instrumentation facility.

Notes and references

1 United Nations Environment Programme, 2022 Global Status Report for Buildings and Construction: Towards a Zero-emission, Efficient and Resilient Buildings and Construction Sector, 2022.
2 M. Haneef, L. Ceseracciu, C. Canale, I. S. Bayer, J. A. Heredia-Guerrero and A. Athanassiou, *Sci. Rep.*, 2017, **7**, 41292.
3 M. Jones, T. Huynh, C. Dekiwadia, F. Daver and S. John, *J. Bionanosci.*, 2017, **11**, 241–257.
4 M. Zhang, Z. Zhang, R. Zhang, Y. Peng, M. Wang and J. Cao, *Composites, Part B*, 2023, **266**, 111003.
5 M. G. Pelletier, G. A. Holt, J. D. Wanjura, E. Bayer and G. McIntyre, *Ind. Crops Prod.*, 2013, **51**, 480–485.
6 S. Bitting, T. Derme, J. Lee, T. Van Mele, B. Dillenburger and P. Block, *Biomimetics*, 2022, **7**, 44.
7 S. Camere and E. Karana, *J. Cleaner Prod.*, 2018, **186**, 570–584.

8 K. K. Alaneme, J. U. Anaele, T. M. Oke, S. A. Kareem, M. Adediran, O. A. Ajibuwa and Y. O. Anabaranze, *Alexandria Eng. J.*, 2023, **83**, 234–250.
9 A. Bhardwaj, J. Vasselli, M. Lucht, Z. Pei, B. Shaw, Z. Grasley, X. Wei and N. Zou, *Manuf. Lett.*, 2020, **24**, 96–99.
10 A. Bhardwaj, A. M. Rahman, X. Wei, Z. Pei, D. Truong, M. Lucht and N. Zou, *J. Manuf. Mater. Process.*, 2021, **5**, 112.
11 E. Elsacker, E. Peeters and L. De Laet, *Sustain. Futures*, 2022, **4**, 100085.
12 A. Mohseni, F. R. Vieira, J. A. Pecchia and B. Gürsoy, *Biomimetics*, 2023, **8**, 257.
13 E. Soh, Z. Y. Chew, N. Saeidi, A. Javadian, D. Hebel and H. Le Ferrand, *Mater. Des.*, 2020, **195**, 109058.
14 S. C. Shen, N. A. Lee, W. J. Lockett, A. D. Acuil, H. B. Gazdus, B. N. Spitzer and M. J. Buehler, *Mater. Horiz.*, 2024, **11**, 1689–1703.
15 B. Modanloo, A. Ghazvinian, M. Matini and E. Andaroodi, *Biomimetics*, 2021, **6**, 68.
16 A. C. S. Lim and M. R. Thomsen, in *eCAADe 2021: Towards a new, configurable architecture*, 2021, pp. 85–94.
17 D. Luo, J. Yang and N. Peek, *3D Print. Addit. Manuf.*, 2025, 3dp.2023.0342.
18 S. Gantenbein, E. Colucci, J. Käch, E. Trachsel, F. B. Coulter, P. A. Rühs, K. Masania and A. R. Studart, *Nat. Mater.*, 2023, **22**, 128–134.
19 E. Soh, J. H. Teoh, B. Leong, T. Xing and H. Le Ferrand, *Mater. Des.*, 2023, **236**, 112481.
20 N. Lin, A. Taghizadehmakoei, L. Polovina, I. McLean, J. C. Santana-Martínez, C. Naese, C. Moraes, S. J. Hallam and J. Dahmen, *ACS Appl. Bio Mater.*, 2024, **7**, 2982–2992.
21 J. H. Teoh, E. Soh and H. Le Ferrand, *IJB*, 2024, 3939.
22 A. M. Rahman, C. O. Bedsole, Y. M. Akib, J. Hamilton, T. T. Rahman, B. D. Shaw and Z. Pei, *Biomimetics*, 2024, **9**, 251.
23 S. Ji and M. Guvendiren, *Front. Bioeng. Biotechnol.*, 2017, **5**, 23.
24 H. Lindemann, A. Fromm, J. Ott and H. Kloft, in Proceedings of IASS Annual Symposia, International Association for Shell and Spatial Structures (IASS), 2017, vol. 2017, pp. 1–8.
25 K.-K. Yun, P. Choi and J. H. Yeon, *Constr. Build. Mater.*, 2015, **98**, 884–891.
26 X. Liu, Q. Li, L. Wang, F. Wang and G. Ma, *Cem. Concr. Compos.*, 2022, **133**, 104688.
27 K. H. Khayat, W. Meng, K. Vallurupalli and L. Teng, *Cem. Concr. Res.*, 2019, **124**, 105828.
28 P. D. Aher, Y. D. Patil, S. M. Waysal and A. M. Bhoi, *Mater. Today Proc.*, 2023, S2214785323040828.
29 J.-W. Rhim and P. K. W. Ng, *Crit. Rev. Food Sci. Nutr.*, 2007, **47**, 411–433.
30 V. Kola and I. S. Carvalho, *Food Biosci.*, 2023, **54**, 102860.
31 A. T. Noguerol, M. Marta Igual and M. J. Pagán, *Food Hydrocolloids*, 2022, **122**, 107108.
32 B. Ilman and A. P. Balkis, *J. Build. Eng.*, 2023, **76**, 107220.
33 J. V. González-Aviña, M. Hosseinpoor, A. Yahia and A. Durán-Herrera, *Cem. Concr. Compos.*, 2024, **146**, 105409.
34 E. Norström, L. Fogelström, P. Nordqvist, F. Khabbaz and E. Malmström, *Ind. Crops Prod.*, 2014, **52**, 736–744.
35 B. Duan, *Ann. Biomed. Eng.*, 2017, **45**, 195–209.
36 A. Farahnaky, H. Askari, M. Majzoobi and Gh Mesbahi, *J. Food Eng.*, 2010, **100**, 294–301.
37 M. Farzi, M. S. Yarmand, M. Safari, Z. Emam-Djomeh and M. A. Mohammadifar, *Int. J. Biol. Macromol.*, 2015, **79**, 433–439.
38 K. Jedvert and T. Heinze, *J. Polym. Eng.*, 2017, **37**, 845–860.
39 D. Zhao, S. Yu, B. Sun, S. Gao, S. Guo and K. Zhao, *Polymers*, 2018, **10**, 462.
40 J. Zhang, W. Xia, P. Liu, Q. Cheng, T. Tahi, W. Gu and B. Li, *Mar. Drugs*, 2010, **8**, 1962–1987.
41 T. Poinot, M.-C. Bartholin, A. Govin and P. Grosseau, *Cem. Concr. Res.*, 2015, **70**, 50–59.
42 M. Geremew Kassa, D. Alemu Teferi, A. M. Asemu, M. T. Belachew, N. Satheesh, B. D. Abera and E. G. Erku, *CYTA J. Food*, 2024, **22**, 2409174.
43 R. Masood, T. Hussain, M. Miraftab, A. Ullah, Z. Ali Raza, T. Areeb and M. Umar, *J. Ind. Text.*, 2017, **47**, 20–37.
44 P. S. Agarwal, S. Poddar, N. Varshney, A. K. Sahi, K. Y. Vajanthri, K. Yadav, A. S. Parmar and S. K. Mahto, *J. Biomater. Appl.*, 2021, **35**, 1132–1142.
45 P. Q. Nguyen, N. D. Courchesne, A. Duraj-Thatte, P. Praveschotinunt and N. S. Joshi, *Adv. Mater.*, 2018, **30**, 1704847.
46 J. Vergara, H. S. Teixeira, C. M. De Souza, J. A. Ataide, F. De Souza Ferraz, P. G. Mazzola and L. F. Mourão, *J. Food Sci. Technol.*, 2022, **59**, 3627–3633.
47 E. W. Van Wijngaarden, A. G. Goetsch, I. L. Brito, D. M. Hershey and M. N. Silberstein, *Soft Matter*, 2024, **20**, 6399–6410.
48 B. Kruppa, G. Strube and C. Gerlach, in *Optical Measurements: Techniques and Applications*, ed. F. Mayinger and O. Feldmann, Springer Berlin Heidelberg, Berlin, Heidelberg, 2001, pp. 99–116.
49 E. Manual, *Engineer*, 1993, vol. 20020626, p. 123.
50 C09 Committee.
51 M. A. Shakir and M. I. Ahmad, *Biofuels, Bioprod. Biorefin.*, 2024, **18**, 1739–1754.
52 N. Lagoueyte and P. R. Paquin, *Food Hydrocolloids*, 1998, **12**, 365–371.
53 P. Di Martino, *AIMS Microbiol.*, 2018, **4**, 274–288.
54 M. Kacuráková, *Carbohydr. Polym.*, 2000, **43**, 195–203.
55 Y. Ren, G. E. Yakubov, B. R. Linter, W. MacNaughtan and T. J. Foster, *Food Hydrocolloids*, 2020, **104**, 105737.
56 A. I. Barzic, in *Polysaccharides*, ed. Inamuddin, M. I. Ahamed, R. Boddula and T. Altalhi, Wiley, 1st edn, 2021, pp. 367–383.
57 S. Zhu, Y. Jin, C. Wei, Q. Yang, Z. Wei, H. Song, S. Liu, Y. Ding and X. Zhou, *Int. J. Food Sci. Technol.*, 2024, **59**, 3781–3790.
58 Q. Fu, R. Liu, L. Zhou, J. Zhang, W. Zhang and R. Wang, *Food Control*, 2022, **134**, 108716.
59 M. Vela-Albarrán, J. Santos, N. Calero, F. Carrillo and L. A. Trujillo-Cayado, *Food Bioprocess Technol.*, 2025, **18**, 6365–6377.

60 A. M. Ribeiro, B. N. Estevinho and F. Rocha, *Food Hydrocolloids*, 2021, **121**, 106998.
61 X. Zhang, Q. Wang, Z. Liu, L. Zhi, B. Jiao, H. Hu, X. Ma, D. Agyei and A. Shi, *Food Hydrocolloids*, 2023, **144**, 109008.
62 Q. Fu, L. Zhou, H. Shi, R. Wang and L. Yang, *Front. Nutr.*, 2023, **10**, 1125312.
63 W. Geng, M. Tian, X. Zhang, M. Song, X. Fan, M. Li, Y. Ma, S. Benjakul and Q. Zhao, *Foods*, 2024, **13**, 3703.
64 V. Singh, S. Indoria, K. J. Jisha and R. L. Gardas, in *Polysaccharides*, ed. Inamuddin, M. I. Ahamed, R. Boddula and T. Altalhi, Wiley, 1st edn, 2021, pp. 325–336.
65 M. Farzi, M. S. Yarmand, M. Safari, Z. Emam-Djomeh and M. A. Mohammadifar, *Int. J. Biol. Macromol.*, 2015, **79**, 433–439.
66 P. Shah and M. M. Driscoll, *Soft Matter*, 2024, **20**, 4839–4858.
67 M. H. Biroun, L. Haworth, H. Abdolnezhad, A. Khosravi, P. Agrawal, G. McHale, H. Torun, C. Semprebon, M. Jabbari and Y.-Q. Fu, *Langmuir*, 2023, **39**, 5793–5802.
68 A. Jha, P. Chantelot, C. Clanet and D. Quéré, *Soft Matter*, 2020, **16**, 7270–7273.
69 J. Guillemenet, S. Bistac and J. Schultz, *Int. J. Adhes. Adhes.*, 2002, **22**, 1–5.
70 S. Sun, M. Li and A. Liu, *Int. J. Adhes. Adhes.*, 2013, **41**, 98–106.
71 D. Araújo, V. D. Alves, J. Campos, I. Coelhoso, C. Sevrin, C. Grandfils, F. Freitas and M. A. M. Reis, *Int. J. Biol. Macromol.*, 2016, **92**, 383–389.
72 T. Todorovic, D. Demircan, J. Ekström, L. Hjelm, E. Malmström and L. Fogelström, *Ind. Crops Prod.*, 2024, **208**, 117841.
73 R. Kivelä, L. Pitkänen, P. Laine, V. Aseyev and T. Sontag-Strohm, *Food Hydrocolloids*, 2010, **24**, 611–618.
74 J. Floury, A. Desrumaux, M. A. V. Axelos and J. Legrand, *Food Hydrocolloids*, 2002, **16**, 47–53.
75 F. Harte and R. Venegas, *J. Texture Stud.*, 2010, **41**, 49–61.
76 W. Sun, M. Tajvidi, C. Howell and C. G. Hunt, *Composites, Part A*, 2022, **161**, 107125.
77 P. N. Ngemakwe, M. Le Roes-Hill and V. Jideani, *Food Sci. Technol. Int.*, 2015, **21**, 256–276.
78 B. Filipčev, M. Pojić, O. Šimurina, A. Mišan and A. Mandić, *LWT*, 2021, **151**, 112156.
79 X. Liu, *J. Appl. Packag. Res.*, 2024, **16**, 3.
80 S. Saporta, F. Yang and M. Clark, *Structures Congress 2015*, 2015, pp. 1253–1265.
81 M. R. Islam, G. Tudryn, R. Bucinell, L. Schadler and R. Picu, *J. Mater. Sci.*, 2018, **53**, 16371–16382.
82 E. Elsacker, M. Zhang and M. Dade-Robertson, *Adv. Funct. Mater.*, 2023, **33**, 2301875.
83 G. Skripkiunas, E. Karpova, G. Yakovlev and A. Ignateva, in 5th International Conference "Nanotechnologies". Abstracts, 2018, pp. 170–170.
84 A. Van Wylick, E. Elsacker, L. L. Yap, E. Peeters and L. De Laet, *Constr. Technol. Archit.*, 2022, **1**, 652–659.